JOURNAL OF MATERIALS SCIENCE 28 (1993) 4693–4703

Autostresses induced by point defects in sintering phenomena: effect on mass transport and sintering stress

D. BERUTO, M. CAPURRO*
*Inter-department Center of Materials Engineering, Istituto di Chimica, and *Istituto di Scienza delle Costruzioni, Faculty of Engineering, University of Genoa, Italy*

States of anelastic strain can be associated with excess concentrations of point defects, as generated by mass transport in a sintering compact. Correspondingly, states of mechanical long-range self-equilibrated stresses ("*autostresses*") can be produced. The relationships between anelastic strain and autostresses have been derived for a two-particle model. A generalized relation between chemical potentials and autostresses, including surface stresses, is provided, which allows derivation of local thermodynamic driving forces for mass transport. The concept of equivalent external sintering stress, assumed to be the driving force for the global densification process, is shown to correspond, approximately, to the material- and history-dependent normal autostress component acting on the neck cross-sections. Predictions made from the model provide a new interpretation of experimental observations of the effect of gaseous phases, such as H_2O and CO_2, on the sintering of MgO and CaO powders.

1. Introduction

It is recognized [1–5] that inhomogeneities, such as particles of different size, asymmetric neck formation, macropores, inclusions, etc., in a sintering compact give rise to differential rates of sintering, i.e. to inhomogeneous strain, which can produce states of internal stresses.

Defay and Prigogine [6] remarked that in a single grain undergoing diffusional processes, the lattice can be deformed with respect to its equilibrium configuration by any local excess of point defects capable of altering the atomic spacings. Novick and Berry [7] have associated the presence of point defects with a local straining of the lattice, showing that a readjustment of such defects under the action of diffusion mechanisms may be responsible for an effect of elastic relaxation.

On this basis, it is possible that inhomogeneous strain arises also on an intermediate scale, between the different regions (bulk, free surfaces and grain boundaries) of a pair or a cluster of sintering particles, on account of differences in the local point-defect concentrations. It is this scale of strain inhomogeneities and their influence on sintering which will be examined in the present paper.

As in the macroscopic case, the microscopic differential strains between free surfaces, interfaces and bulk, during densification processes, can give rise, by mutual constraint, to mechanical long-range internal stresses. In the absence of external load, such internal stresses will here be called "autostresses". In a surface or interfacial layer the autostress tensor tends to become tangential to the surface [6] and so reduces to a two-dimensional "surface stress" tensor.

Surface stress in solids, as pointed out, for example, by Herring [8] and Shuttleworth [9], is not the same as surface energy in concept and value. Solliard and Flueli [10] have measured the surface stress of small metal particles, while Nicolson [11] showed both theoretically and experimentally that in some small ionic crystals the surface stress can exceed the value of surface energy by a factor of over 5.

All these works [8–11] examined phenomena which resulted from elastic strain in the surface: in such cases the surface stress is locally related to the partial derivative of the surface energy with respect to the elastic strain. When the strain is anelastic and history-dependent, as it is the case in compacts during sintering [12], the stress–strain relations both of surfaces and of the bulk are more complex and depend on the instantaneous geometry of the entire system. In the present work, such relationships are derived from a generalization of the mechanical model of a surface layer. The generalized model is used to calculate expressions for the autostresses in the grain boundary, in the free surface and in the bulk of a sintering two-particle system.

Transport due to diffusive flux between different regions of a system is driven by the gradient of the chemical potential of the diffusing species, which is known to be related locally to the normal stress [13, 14]. A generalization of this statement will be obtained in this paper showing that the complete stress tensor, including the two-dimensional stresses in

0022–2461

a surface or interface layer, contributes to the chemical potential.

Most recent theories on sintering of powders and porous compacts envisage the densification rate as the product of a kinetic factor, a microstructural factor and a global driving force, eventually accessible to experiment and termed "sintering stress" [1, 13], "sintering pressure" [15] or "sintering potential" [14, 16]. A very important question, not yet completely answered, is the relationship of the sintering stress to the internal properties of the system. In this paper the question is widely debated and a material- and history-dependent parameter, related to the autostresses, is suggested to represent, at least in a first approximation, the experimental concept of equivalent sintering stress.

Experimental observations of the catalytic effect of gaseous phases, such as water vapour and CO_2, on the sintering of MgO and CaO powders, suggest that a gaseous phase, to be a catalyst, must not only be chemically adsorbed at the surface, but also dissolve into the inner surface layer. These results can be explained by the nature of the autostresses as derived in this paper.

2. The nature of internal stresses induced by point defects

As a matter of definition, the standard undeformed state of a crystalline solid can be assumed to coincide with its configuration at thermodynamic equilibrium. Accordingly, if an excess of point defects, with respect to the equilibrium concentrations, is created in a sufficiently large region of the solid, by diffusion or other processes, a state of deformation is introduced. This deformation may be prevented in part or totally, depending on the geometrical constraints which exist between the different regions of the solid.

The resulting state of strain at each location, according to Nowick and Berry [7], can be described in a continuum approach by a symmetric tensor field, which is proportional to the amount of defects per unit volume exceeding the equilibrium concentration in that place.

It will be convenient to define separately defect-induced strains in a three-dimensional lattice and at surface or grain boundaries, by

$$\boldsymbol{E}(i) = n_{vi}\Omega_o \boldsymbol{L}_v(i) \tag{1a}$$

$$\varepsilon(i) = n_{si}\Omega_s L_s(i) \tag{1b}$$

where $\boldsymbol{E}(i)$ and $\varepsilon(i)$ represent, respectively, a three-dimensional strain tensor for the bulk and a corresponding two-dimensional tensor for a surface or grain boundary; n_{vi} and n_{si} are, respectively, the bulk and surface excess concentrations (with respect to the unstrained state) of defects belonging to a species (i); Ω_o and $\Omega_s = \Omega_o/d_s$ are, respectively, the atomic volume and the atomic area, where d_s is the thickness of the surface layer. It should be remembered that, at equilibrium, the defect concentrations in the surface, grain boundary and bulk, differ from each other. The excess quantity in, for example, the surface, is defined relative to the concentration which would be present when the net exchange of atoms between that region and regions of different bonding environments is zero [17].

The tensors $\boldsymbol{L}_v(i)$ and $\boldsymbol{L}_s(i)$ are the products of shape factors (i.e. of factors which depend on the defect symmetry with respect to the symmetry of the lattice) and of distribution functions which account for the spatial distribution of the defect population within the region considered. For vacancies, the symmetry factor will have principal components of negative sign, with values between 0 and -1; for interstitials, the principal components will be positive. The distribution factors will always be different from zero and of the order of unity for distributions approaching isotropy.

States of stress can result from states of strain described by Equation 1 if the region considered cannot deform freely, i.e. is constrained. A simple example in which a stress can be created is that of an isolated single particle under non-equilibrium conditions obtaining when matter is exchanged with the environment across its surface. Under these circumstances, the defect concentration at the surface can be different from the equilibrium value. If the surface becomes enriched in vacancies, it would shrink by an amount given by Equation 1b, provided that it is free to do that. Actually the surface, being connected to the bulk, cannot slide freely, therefore it will be stressed in tension, while exerting on the bulk a radial compression. The amount of such stresses depends on the elastic compliances of both the surface and the bulk and can be calculated easily in the case of spherical symmetry.

The example shows how true mechanical stresses can exist in the surface of a crystal when defect inhomogeneities are present. Experimental evidence of this behaviour has been reported by Nicolson [11], who observed by X-diffraction methods the reduction of the crystal parameter connected with the adsorption of gas at the surface of very fine crystalline powders. The effect was observed also for H_2O on MgO [18].

During the sintering process, two or more particles weld together at grain boundaries, thus exerting mutual constraints on one another. If the excess point-defect concentrations due to mass transport turn out to be different in the different regions of the system, we must expect that states of internal stresses (autostresses), globally in mechanical equilibrium, will be produced in the bulk as well as in the surface and boundary layers.

3. Mechanical model of the surface and interface

From the mechanical point of view, a stressed surface layer can be described, following the theory of two-dimensional structures [19], as a membrane of vanishing thickness. The membrane is made mechanically equivalent to the layer, by applying convenient stress resultants to represent the through-thickness state of stress.

On the outer and inner side of the membrane , with outwardly normal vectors respectively $^{+}\boldsymbol{n}$ and $^{-}\boldsymbol{n}$, the

tractions $\boldsymbol{nS}^+$ and $-\boldsymbol{nS}^-$, generated by the bulk stress tensors $\boldsymbol{S}^+$ and $\boldsymbol{S}^-$, at the boundaries of the layer, act as external loads. Inside the membrane, stresses can result which have components both tangent and normal to the surface. However, because the solids considered here follow a Cauchy model, without couple-stresses [20], moment resultants could arise in the layer only from through-thickness stress distributions. Then all moment resultants can be assumed to vanish, if referred to a given "mean surface", located at a distance z_o ($z_o < d$) from the layer bottom. In such conditions the solid surface obeys a Gibbs model [6].

Letting the equivalent membrane coincide with the mean surface as defined above, shear resultants will vanish together with moments and all membrane stresses will lie in the plane tangential to the surface. Then the membrane stress tensor is two-dimensional, and described by

$$\sigma = \int_o^d \boldsymbol{S}_s \mathrm{d}z \tag{2}$$

where $\boldsymbol{S}_s$ represents the in-plane projection of the three-dimensional stress tensor $\boldsymbol{S}$ originally present in the layer.

At any given point of the idealized membrane, the membrane stress tensor, σ, must fulfil two local equilibrium equations [21], Equations (3) and (4):

$$\nabla_s \sigma = \boldsymbol{t}^- - \boldsymbol{t}^+ \tag{3}$$

for in-plane equilibrium, where ∇_s is the gradient operator on the surface and $\boldsymbol{t}^+$ and $\boldsymbol{t}^-$ represent the tangent loads eventually carried by the two bulk phases

$$\sigma : \boldsymbol{K} = p^+ - p^- \tag{4}$$

for equilibrium in the direction of the normal. Equation 4 is equivalent to Laplace's equation for solids, on a scale where faceting can be neglected; $\boldsymbol{K}$ is the curvature tensor and the operational symbol ":" indicates matrix scalar product; p^+ and p^- are the loads applied normal to the two sides of the membrane, given by, respectively

$$p^+ = \boldsymbol{nS}^+\boldsymbol{n} \tag{5a}$$

$$p^- = \boldsymbol{nS}^-\boldsymbol{n} \tag{5b}$$

If $\boldsymbol{t}^+ = \boldsymbol{t}^-$, and if the membrane stress tensor is isotropic, i.e. $\sigma = \sigma \mathrm{I}$, Equation 3 predicts constancy for σ through the entire surface. In such a case the behaviour of the layer is quite similar to that of a liquid.

The mechanical work expended to strain a volume of the solid not containing interfaces, is expressed by the volume integral

$$\mathrm{d}W = \int_V \boldsymbol{S} : \mathrm{d}\boldsymbol{E}\, \mathrm{d}V \tag{6}$$

of the scalar product between the stress tensor and the increment of total strain $\mathrm{d}\boldsymbol{E}$.

The work expended to strain a surface or grain boundary, including the work required for surface creation and annihilation, reads

$$\mathrm{d}W_s = \int_s (\sigma : \mathrm{d}\varepsilon + p^+ du^+ + p^- \mathrm{d}u^-)\mathrm{d}A \tag{7}$$

where $\mathrm{d}\varepsilon$ is the total strain increment of the memrane, including defect-induced strain as expressed by Equation 1; du^+ and du^- are the displacements at the two sides of the membrane, in the direction of the normal.

Indicating by $\mathrm{d}\varepsilon^+$ and $\mathrm{d}\varepsilon^-$ the incremental axial strain components in the direction of the normal, respectively, at the outer and inner boundaries of the surface layer, we can write approximately (for small z_o, d)

$$du^+ = (\mathrm{d} - z_o)\, \mathrm{d}\varepsilon^+ \tag{8a}$$

$$du^- = z_o \mathrm{d}\varepsilon^- \tag{8b}$$

Bulk quantities such as $\mathrm{d}\varepsilon^+$ and $\mathrm{d}\varepsilon^-$ are thus involved in the surface work, in accord with the fact that the membrane properties depend on the interaction of the surface or boundary with the bulk solid.

4. Calculation of the autostresses in a two-particle system during sintering

The model in Fig. 1 illustrates the standard idealization for a pair of single-crystal particles during isothermal sintering. The gradients in vacancy concentration produced by diffusion of atoms from the bulk to the adjacent grain boundary, i.e. the gradients in excess vacancy concentrations, can be expected to relax the elastic bonds of the boundary layer, giving rise to an anelastic negative strain ε_b, approximately isotropic and homogeneous. If the grain boundary is not free to deform, a tensile stress corresponding to the elastic part of ε_b will appear and the effective strain will be less than ε_b.

The surfaces of the two particles in the neck regions may exchange matter with the grain boundary or with other phases, both solid and gaseous.

These transport phenomena modify the point-defect concentrations and, therefore, it is possible to define two isotropic anelastic strains ε_1 and ε_2 for the corresponding membranes. Magnitudes and signs of such strains will depend on the excess of point defects

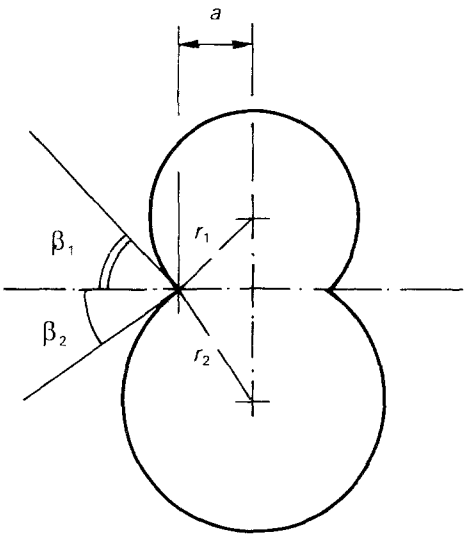

Figure 1 Idealized model of a two-particle system.

and their kind. If, for instance, the surfaces receive atoms in interstitial sites, both strains will be positive; if an excess of vacancies is produced, the unrelaxed strains will be negative. The signs and magnitudes of the corresponding membrane stresses will depend on the surface constraints and will be related to the elastic compliances of the system.

A convenient model to describe the above situation consists of three membranes, meeting at a triple joint and enveloping two obtruncated spheres. The autostresses in the region of the neck can then be calculated following a standard method for internally constrained structures [22]. The underlying concept can be better understood if referred to a simple in-plane truss model (Fig. 2), in which the bars represent the three membranes as they meet at the neck. Now imagine disconnecting the grain boundary (represented by bar b in Fig. 2b) along the joint periphery. Let bar b undergo a negative stretch, equal to the unrelaxed anelastic shrinkage, ε_b, of the grain boundary. While the free end of the bar tends to depart from the joint, the corner formed by the remaining pair of bars, will either follow or oppose the displacement, depending on whether bars 1 and 2 are themselves positively or negatively strained.

Because the net displacement of the joint (point O in Fig. 2b) must be zero to maintain the continuity of the system, the net anelastic shift δ must balance the algebraic resultant of elastic displacements at the end of bar b and at the corner of the simple truss 1 + 2.

The elastic displacements are produced, respectively, by a membrane stress σ_b in the grain boundary and by membrane stresses σ_1 and σ_2, which act in the two envelopes and equilibrate with σ_b. No point force can be exchanged with the bulk at the triple joint.

Defining the elastic rigidities as k_b and k_s, respectively, for the grain boundary and for the "simple truss" formed by membranes 1 and 2, the compatibility equation reads

$$\delta = \sigma_b(1/k_s + 1/k_b) \tag{9}$$

But the net shift, δ, is also given by

$$\delta = \delta_b + \delta_s \tag{10}$$

where δ_b and δ_s are, respectively, the anelastic displacements of the boundary and of the truss corner.

In the grain-boundary membrane, which can be regarded as a circular plate of radius a, the radial displacement, δ_b, is related to surface shrinkage, ε_b (supposed to be homogeneous and isotropic), by the simple equation

$$\delta_b = \varepsilon_b a/2 \tag{11}$$

as readily obtained by elementary geometry. Under similar conditions, as outlined in Appendix 1, the membranes which surround the two particles, will shrink at the triple joint by approximately the amount

$$\delta_s \approx (\varepsilon_1 + \varepsilon_2)a/4 \tag{12}$$

Equations 11 and 12 allow one to calculate δ; according to Equation 10 the elastic rigidities k_s and k_b are also required in order to solve for σ_b. Values of k_s, k_b, as calculated for spherical particles, are given in Appendices 2 and 3; they are found to depend on the elastic constants G_s and G_b of the membranes, as well as on the angles β_1 and β_2. After eliminating k_s and k_b, Equation 11 yields

$$\sigma_b = -G^*(\varepsilon_b + \varepsilon_s)/2 \tag{13}$$

where

$$G^* = \frac{2G_s G_b}{[G_b(\sin^2\beta_1 + \sin^2\beta_2)/\sin^2(\beta_1 + \beta_2) + 2G_s]} \tag{14}$$

From equilibrium of the triple joint (Fig. 2c), comes

$$\sigma_1 = \sigma_b \sin\beta_2/\sin(\beta_1 + \beta_2) \tag{15a}$$

$$\sigma_2 = \sigma_b \sin\beta_1/\sin(\beta_1 + \beta_2) \tag{15b}$$

In the special instance of equal-size particles ($\beta_1 = \beta_2 = \beta$), Equations 14 and 15 become

$$G^* = 4G_s G_b \cos^2\beta/(G_b + 4G_s\cos^2\beta) \tag{16}$$

$$\sigma_1 = \sigma_2 = \sigma_b/2\cos\beta \tag{17}$$

The relationship between the surface stresses (σ_b, σ_1, etc.) and the surface tensions, Γ_s and Γ_b, follow directly if the membrane elasticities G_b and G_s are expressed in terms of Young's modulus which, in turn,

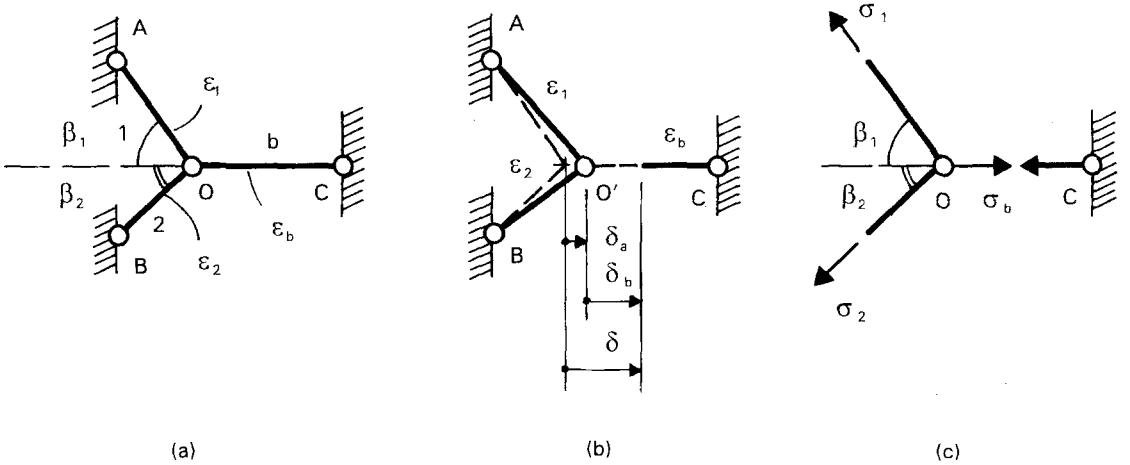

(a) (b) (c)

Figure 2 Elastic-truss model for triple joint of two particles at a boundary (a) geometric model; (b) displacements in the free-body configuration; (c) internal stresses.

can be related to the surface tension. In fact, G_b and G_s can be defined by, respectively, $G_b = E_b d_b/2(1 + \nu)$ and $G_s = E_s d_s/2(1 + \nu)$, where d_b and d_s are the thicknesses of the layers, E is the elastic modulus of the material and ν Poisson's ratio, which usually ranges between 0.25 and 0.35 [23], and in this case is set equal to $\nu \approx 0.27$. As a first approximation, the Young's modulus, E, is given by $E \approx \pi^2\Gamma/b$ or by a similar expression [24], where b is the atomic spacing. Accordingly, σ_b can be expressed as

$$\sigma_b = -\left[\frac{\pi^2 d_b}{(1 + \nu)b}\right]\left[\frac{\Gamma_b \cos^2\beta}{(\Gamma_b d_b/\Gamma_s d_s) + 4\cos^2\beta}\right](\varepsilon_b + \varepsilon_s) \tag{18}$$

If the thickness of the free surface is assumed to be the same as that of the grain boundary and if the ratio Γ_b/Γ_s is less than unity [13], at the beginning of sintering, Equation 18 simplifies to

$$\sigma_b \approx -\frac{\pi^2 d_b}{4(1 + \nu)b}\Gamma_b(\varepsilon_b + \varepsilon_s) \approx \sqrt{2}(d_b/b)\Gamma_b(\varepsilon_b + \varepsilon_s) \tag{19}$$

Thus the grain-boundary stress, σ_b, turns out to be directly proportional to the corresponding grain-boundary tension Γ_b, which, in fact, has been considered by some authors [16] to be equivalent to a constant mechanical traction. However, it should be emphasized that the magnitude and even the sign of the surface stress, which is the proper mechanical variable, are also proportional to the defect-induced *anelastic* strains, which can change during the process.

Because the grain boundary is a vacancy sink, ε_b is always negative and relatively large in absolute value, and because, in most cases, ε_s is negative or zero, the grain-boundary stress is normally tensile. But, in certain cases, the magnitude of σ_b can be decreased by the formation of positive strains at the neck surface and it is possible to envisage a situation in which the total strain is such as to make σ_b equal to zero or even negative. Negative values of σ_b might occur when gases adsorb in the surface layer, leading to a positive ε_s.

Membrane stresses σ_1 and σ_2 in the surfaces enveloping the two particles, are themselves tensile for values of β in the range from 0 to $\pi/2$ and would become compressive only for a convex neck surface ($\beta > \pi/2$). The situation corresponding to $\beta = \pi/2$ cannot be in equilibrium, unless with $\sigma_b = 0$.

Knowledge of the surface stresses allows calculation of the bulk stresses that act on the neck cross-section. Suppose that one of the two particles (say grain 1) is disconnected from the grain boundary (Fig 3), very close to the joint. In order to keep mechanical equilibrium, the membrane stress σ_1 must be applied to the joint, and the bulk stresses to the neck cross-section.

If the neck has an approximately circular cross-section and is axially symmetric (i.e. if β_1 is nearly constant along the joint periphery), the bulk resultant is normal to the grain boundary and is given by

$$f_n = 2\pi a\,\sigma_1 \sin\beta_1 \tag{20}$$

being applied at the centre-of-area of the grain-boundary cross-section. Accordingly, the bulk of particle

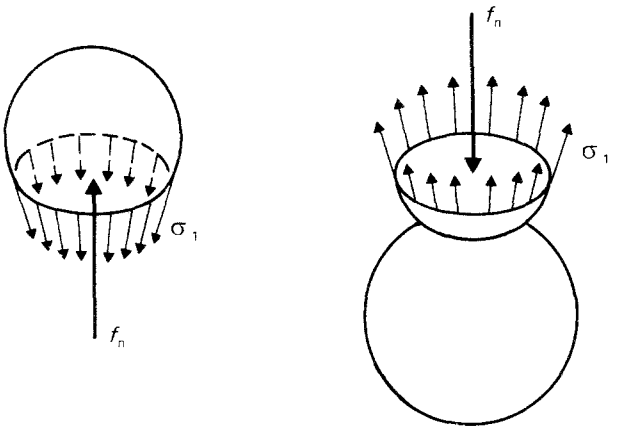

Figure 3 Visualization of resultant bulk stress.

1 adjacent to the boundary, is subjected to a normal compressive stress, S_{nn}, which, in the mean, amounts to

$$S_{nn} = -\frac{2\sigma_b \sin\beta_1 \sin\beta_2}{a \sin(\beta_1 + \beta_2)} \tag{21}$$

as obtained by eliminating σ_1 in Equation 20 via Equations 13 and 15 and dividing by the cross-sectional area, πa^2.

In the case of identical particles ($\beta_1 = \beta_2$), substitution of σ_b from Equation 18, yields

$$S_{nn} = \left[\frac{\pi^2 d_b}{(1 + \nu)b}\right]\frac{\Gamma_b}{r}\left[\frac{\cos\beta}{(\Gamma_b d_b/\Gamma_s d_s + 4\cos^2\beta}\right](\varepsilon_b + \varepsilon_s) \tag{22}$$

where r is the radius of a particle and $a = r \sin\beta$.

At the beginning of the sintering process (i.e. $\beta = 0$), under the above assumptions, S_{nn} approaches the value

$$S_{nn} = \frac{2\Gamma_b}{r_o}\frac{d_b}{b}(\varepsilon_b + \varepsilon_s) \tag{23}$$

Distributions of S_{nn} over the neck cross-section have been calculated by several authors (e.g. [2, 4, 13]) from the condition $\nabla^2 S_{nn} = \text{const}$, and found to be, for this and for other simple models, parabolic in shape.

In general, depending on the geometrical shape, the resultant of σ_1 on the joint periphery may have also a component tangential to the grain boundary and, furthermore, may exhibit an eccentricity with respect to its centre-of-area. In that case, in addition to a normal force, the boundary may be subjected to shear, bending moments, and a torque. For regular shapes, however, the effect of the normal force is usually more important than the others.

If the grain boundary is flat, the state of stress in the adjoining regions of the two particles is the same. If the boundary is curved, particle 2 receives an additional force from the resultant of the membrane stress acting in the grain boundary.

Accordingly, there will be a difference in the states of stress acting on the two particles, with the particle adjoining the concavity of the boundary undergoing, in the mean, a higher compressive stress.

This unequal stress can affect the grain growth.

5. Driving forces for mass transport and autostresses

Consider, for the sake of simplicity, an elemental solid formed by a bulk phase (v), free-surface layers of thickness d_s and grain-boundary layers of thickness d_b. Free surfaces and grain-boundary layers will be assumed to follow the mechanical model introduced in Section 3, which is equivalent to Gibb's surface model [6]. In this system the species considered to undergo diffusional transport are, for brevity, only lattice atoms and vacancies.

The change in the total Helmholtz free energy of the system is given by

$$dF = dF_v + dF_s + dF_b \tag{24}$$

At constant temperature, T, the change of free energy of a region of the system, say the bulk, is

$$dF_v = \mu_{1,v}^* dN_{1,v} + \mu_{2,v}^* dN_{2,v} + \int_V \boldsymbol{S}:d\boldsymbol{E}\, dV + \delta Q - T dS_v \tag{25}$$

where $dN_{1,v}$ and $dN_{2,v}$ are the changes in numbers, respectively, of atoms and vacancies in the bulk, $\mu_{1,v}^*$, $\mu_{2,v}^*$ are coefficients to be interpreted later, δQ is the heat exchange, and the integral represents the mechanical work.

The mechanical work will be expended, in general, for plastic and elastic deformations as well as for viscous deformation (including creation and annihilation of volume due to the exchange of defects between the bulk and the other regions) which is responsible for densification. On account of the additivity of strain increments, we can write

$$d\boldsymbol{E} = d\boldsymbol{E}_{pl} + d\boldsymbol{E}_{el} + d\boldsymbol{E}_2 \tag{26}$$

where subscripts pl, el indicate, respectively, plastic and elastic strain increments and subscript 2 refers to that part of the total strain that is induced by an excess vacancy concentration $dn_{2,v}$. The contribution of the elastic strain is normally smaller than the anelastic part of the total strain [25], and can be neglected.

Separating the different parts of the total strain increment and taking Equation 1a into account, Equation 25 can be written

$$dF_v = \mu_{1,v}^* dN_{1,v} + \mu_{2,v}^* dN_{2,v} + \int_V \boldsymbol{S}:\boldsymbol{L}_v(2)\Omega_o dn_{2,v} dV + \int_V \boldsymbol{S}:d\boldsymbol{E}_{pl} dV + \delta Q_v - T dS_v \tag{27}$$

By applying the theorem of the mean value to the first integral, we have also

$$dF_v = \mu_{1,v}^* dN_{1,v} + (\mu_{2,v}^* + \bar{\boldsymbol{S}}:\boldsymbol{L}_v(2)\Omega_o) dN_{2,v} + \int_V \boldsymbol{S}:d\boldsymbol{E}_{pl} dV + \delta Q_v - T dS_v \tag{28}$$

where $\bar{\boldsymbol{S}}$ represents the mean stress tensor over the bulk domain V. Because F_v is a function of the state variables $N_{1,v}$ (number of atoms in V) and $N_{2,v}$ (number of vacancies in V), the equality

$$\left(\frac{\partial F_v}{\partial N_{2,v}}\right) dN_{2,v} = (\mu_{2,v}^* + \bar{\boldsymbol{S}}:\boldsymbol{L}_v(2)\Omega_o)\, dN_{2,v} \tag{29}$$

must be true for any arbitrary increment of the vacancy number. Then the relation

$$\bar{\mu}_{2,v} = \mu_{2,v}^* + \bar{\boldsymbol{S}}:\boldsymbol{L}_v(2)\Omega_o \tag{30}$$

is obtained, where $\bar{\mu}_{2,v}$ is the ordinary chemical potential of the bulk vacancies. Accordingly, $\mu_{2,v}^*$ represents the stress-free chemical potential.

Similar equations for surfaces and grain boundaries must take into account the fact that such regions are not autonomous phases.

Following Defay and Prigogine [6], the ordinary chemical potential for vacancies at free surfaces or interfaces is

$$\bar{\mu}_{2,i} = \frac{\partial F_i}{\partial N_{2,i}} + \frac{\partial F_i}{z_o \partial N_{2,v^-}} + \frac{\partial F_i}{(d_i - z_o)\partial N_{2,v^+}} \tag{31}$$

where subscript i (s, b) can identify either a surface or grain boundary and superscripts $-$ and $+$ refer to locations at either of the two sides of a given interface layer.

Equation 31, introduced in equations which describe the free energy balance for the surface and the boundary, yields respectively

$$\bar{\mu}_{2,s} = \mu_{2,s}^* + \bar{\sigma}_s:\boldsymbol{L}_s(2)\Omega_s + (\bar{p}_s^- - \bar{p}_s^+)L_{v,n}(2)\Omega_o \tag{32}$$

and

$$\bar{\mu}_{2,b} = \mu_{2,b}^* + \bar{\sigma}_b:\boldsymbol{L}_b(2)\Omega_b + (\bar{p}_b^- - \bar{p}_b^+)L_{v,n}(2)\Omega_o \tag{33}$$

where $L_{v,n}(2)$ is the component of $\boldsymbol{L}_v(2)$ in the direction normal to the interface. Barred symbols refer, as before, to mean quantities.

Equations 30, 32 and 33 relate the ordinary and the stress-free chemical potentials to the corresponding complete stress tensors in the bulk and in the surfaces/boundaries. Such equations are more complete than those usually adopted in the literature [14], which consider only a part (normally the isotropic component) of the stress tensor.

It should be noted that Equations 30, 32 and 33, even though derived in terms of mean values for the entire system, can be applied to local parts of it, because balance equations like Equation 28 can be assumed to hold also for any arbitrary part of the system. In this case the mean stresses must be replaced by the local stresses and also the chemical potentials of the diffusing atoms must be defined as local quantities. Symbolically this procedure corresponds to removing bars in Equations 30, 32 and 33.

Differences in ordinary chemical potentials arise between any two locations of the system subjected to different states of stress and, in particular, along each path crossing a surface or interface. The difference in potentials, divided by the distance moved (z_o or $d - z_o$, according to circumstances) corresponds to a sort of local free-energy gradient which acts as a localized driving force for mass exchange between the corresponding regions.

The driving forces g_1 and g_2 for the exchanges of vacancies in a system composed by two identical particles, along the paths

1. neck free surface → grain boundary (line 1 in Fig. 4),

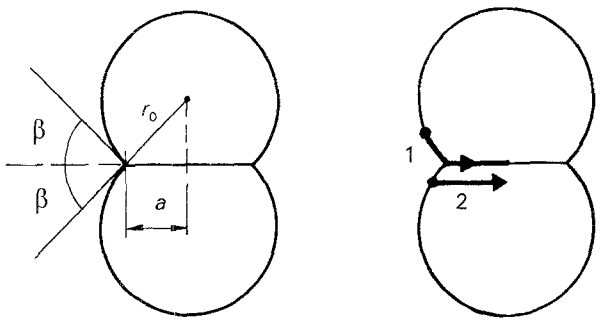

Figure 4 Two-particle system with particles of equal size: examined diffusion paths.

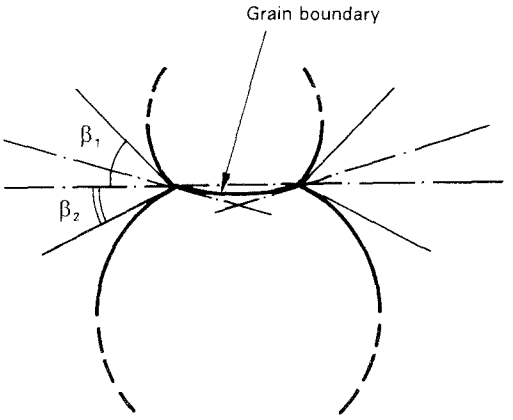

Figure 5 Model for the description of grain-boundary curvature.

2. neck free surface → neck region of the bulk (line 2 in Fig. 4),
are easily obtained from Equations 30, 32 and 33

$$g_1 = \frac{\mu_{2,b}^* - \mu_{2,s}^*}{d_o} - \frac{\sigma_b \Omega_o}{d_o}\left(\frac{1}{d_b} - \frac{1}{2d_s\cos\beta} + \frac{1}{r_n}\right) \quad (35)$$

$$g_2 = \frac{\mu_{2,b}^* - \mu_{2,s}^*}{z_o} - \frac{\sigma_b \Omega_o}{z_o}\left(\frac{1}{d_b} - \frac{1}{2d_s\cos\beta}\right) - \frac{p_o\Omega_o}{z_o} \quad (36)$$

where r_n is the radius of curvature of the neck, $-p_o = p_s^+$ is the pressure of a fluid, which acts upon the free surfaces of the system and $d_o = d_b/2 + z_o$. For the sake of simplicity the tensors $\boldsymbol{L}_i(2)$ $(i$ = v, s, b) have been approximated with negative unit tensors, which would imply perfect isotropy of the lattice and of the defect distribution. Negative signs of gradients g_1 and g_2 imply vacancy transport in the direction of the arrows (Fig. 4) and matter flow in the opposite direction. It should be noticed that the local driving forces consist of two terms, one due to the gradients of the stress-free thermodynamic chemical potentials and the other due to gradients of autostresses. Thus, as one should expect, mass transport can occur in the absence of stress gradients because the differences in the purely thermodynamic, stress-free chemical potentials can be different from zero.

In general, a difference between the states of stress in the bulk and in the surface phases can either increase or decrease the local driving force for mass transport. In particular, for the model being examined

(i) the grain-boundary stress, σ_b, is always tensile (i.e. positive). Accordingly the contribution of the autostresses depends on the signs of the parentheses in Equations 35 and 36;

(ii) for both paths, at the beginning of sintering, $\cos\beta \approx 1$ and therefore the autostresses in all cases help to drive matter to the free surface;

(iii) as sintering proceeds, $\cos\beta$ decreases and the contribution of autostresses to the local driving force is lessened;

(iv) the neck curvature appears as a significant parameter only for path 1, and then only in the initial stage of sintering, when r_n may be of the order of d_s and d_b;

(v) external pressure acts in favour only of path 2.

Under some circumstances, stress gradients can be the only significant driving forces. For example, stress gradients drive mass transport between the bulk phases of two particles separated by a curved grain boundary (Fig. 5) [26]. Curved grain boundaries arise normally when one particle is smaller than its neighbour across the boundary. In this case there is a difference between the stresses, S_{nn}, in the two bulk phases adjoining the boundary. From simple geometrical considerations, letting $\sigma_1 = \sigma_2$ and assuming the stress S_{nn} to act uniformly upon the neck cross-section, we obtain

$$\delta\mu_2 = -2\Omega_o\sigma_b \sin\tfrac{1}{2}(\beta_1 - \beta_2)/a \quad (37)$$

The difference in the dihedral angles β_1 and β_2 increases with the difference in radii r_1 and r_2 of the two particles which are formed across the boundary. If the difference between the radii is not very large, Equation 37 can be approximated by

$$\delta\mu_2 = -\Omega_o\sigma_b\,[(1/r_1) - (1/r_2)] \quad (38)$$

This is a well known result [27] which predicts a flow of matter from the convex side of the boundary toward the concave side, i.e. from the smaller particle to the larger particle, but here the grain-boundary stress replaces the surface energy of the grain boundary.

6. Sintering potential and autostresses

The sintering potential or sintering stress [13–16] has been defined as the equivalent external stress, Σ, to be applied to the system to halt densification. This parameter is quite useful as, under certain conditions, it is accessible to experiment [28].

Among the most significant experimental features of the sintering stress Σ, one may list

(i) it is almost independent on temperature [29];

(ii) it increases almost linearly with increasing green density [30];

(iii) at constant temperature and green density, it decreases as the relative density increases [31].

Furthermore, if the equivalent external sintering stress is understood as an equivalent driving force only for mass-transport processes which produce densification, it seems quite reasonable to assume that

(iv) its value must tend to vanish when the surface diffusion and/or vapourization and condensation are the dominant transport mechanisms.

A very interesting question, not yet completely answered, is the relationship of the sintering stress with the internal properties of the system. Gregg and Rhines [32], Beere [33, 34], De Jonghe and Rahaman [13], Cannon and Carter [14] made important contributions to such understanding, but several questions remain open. For instance, the attempt to define the sintering stress, Σ, as the partial derivative of the total surface energy, F_{s+b} (free surfaces and grain boundaries), with respect to the axial shrinkge [14] implies that the axial shrinkage is regarded as a state variable. This assumption might be questionable because the axial shrinkage includes anelastic and, in certain cases [35], plastic phenomena, which are history-dependent.

Instead of using the concept of partial derivative, some authors define Σ as the ratio of the change in total surface energy, dF_{s+b}, to the change of volume [36]. This definition certainly applies also when the axial shrinkage is not a state variable; however, neither $\delta F_{s+b}/\delta L$ nor $\delta F_{s+b}/\delta V$ are directly related to densification, because, for instance, in the case of a predominant coarsening mechanism, the ratios can be very large, but the densification is negligible.

The mechanical work, which is a part of dF_{s+b}, is directly related to the densification. This can be easily proven, considering that the work done by the autostresses to change and to strain free surfaces and grain boundaries per unit axial shrinkage, equals the work of the autostresses in the bulk, because the total work of the system, in the absence of external forces, must be zero. Thus, for systems approaching the geometry of the model considered in the present paper, the work in the bulk is mainly the product of the resultant f_n of the normal autostress, multiplied by the axial shrinkage (i.e. densification), namely

$$\begin{aligned} dW_{s+b} &= -dW_v \\ &= f_n\, dL \end{aligned} \tag{39}$$

where, in the case of a two-particle model, f_n is given by Equation 20. According to Equation 39, f_n has the meaning of a "sintering force" and the corresponding stress, S_{nn}, on the actual neck cross-section corresponds to an internal "sintering stress".

Equation 21 gives

$$S_{nn} = \left[\frac{\pi^2 d_b}{(1+\nu)b}\right]\frac{\Gamma_b}{r_o} \times \left[\frac{\cos\beta\,(\cos\beta/2)^{2/3}}{(\Gamma_b d_b/\Gamma_s d_s) + 4\cos^2\beta}\right](\varepsilon_b + \varepsilon_s) \tag{40}$$

where r_o is the initial radius of a particle, related through $r = r_o\,(\cos\beta/2)^{-2/3}$ to the actual radius, under the assumptions that total volume and the spherical shape are conserved.

The temperature dependence of S_{nn} is mainly due to the temperature dependence of the surface tension, Γ_b, in Equation 40. As known, the surface tension, at constant composition, decreases only slightly with temperature [27] (in the range of the sintering temperature). Accordingly, the internal sintering stress, S_{nn}, fulfils the requirement of feature (i).

The dependence of S_{nn} on the green density cannot be fully explored with a two-particle model; however, it is apparent that the expression of S_{nn} is strongly related to the initial geometry of the system. In the present case, S_{nn} is inversely proportional to the starting radius of the particle, r_o, in agreement with the derivation of Gregg and Rhines [32]. Furthermore, S_{nn} is nearly a constant for β increasing up to 60°, and decays rapidly in the final phase of sintering, vanishing as $\beta = \pi/2$ as illustrated in Fig. 6. According to the present model, an increase in β corresponds to an increase of the actual relative density and the limiting case $\beta = \pi/2$ indicates the end of densification (feature iii).

The sintering stress defined by Equation 40 also has the important property of vanishing when surface diffusion and/or vapourization and condensation mechanisms are the dominant phenomena (feature iv). In this case, S_{nn} vanishes because the total number of excess vacancies in $\delta N_{2,b}$ and $\delta N_{2,s}$, respectively, in the grain boundary and free surface, obeys $\delta N_{2,b} = -\delta N_{2,s}$. According to Equation 1, this means that the average values of ε_b and ε_s obey the condition $\varepsilon_b + \varepsilon_s = 0$.

The newly defined internal property S_{nn} therefore obeys all the requirements concerning the equivalent external sintering stress, Σ. On this basis, the identity

$$\Sigma = S_{nn} \tag{41}$$

can be tentatively assumed.

It is clear that S_{nn} is dependent upon the geometry of the system. Accordingly, extensive geometrical information on the sample microstructure and its evolution is required to make a quantitative estimate of such a variable.

It should be observed that the definition of S_{nn} given in the present analysis does not correspond to a true thermodynamic potential. This implies that, if Equation 41 holds, the driving force used in describing the rate of densification (e.g. [13]) might depend upon the particular path controlling the process. This seems a reasonable prediction, because different diffusion paths can produce different anelastic strain states.

Furthermore, local mass transports are driven, as we have shown in the previous section, by autostress gradients and by gradients of stress-free chemical potentials. Accordingly, the global equivalent driving

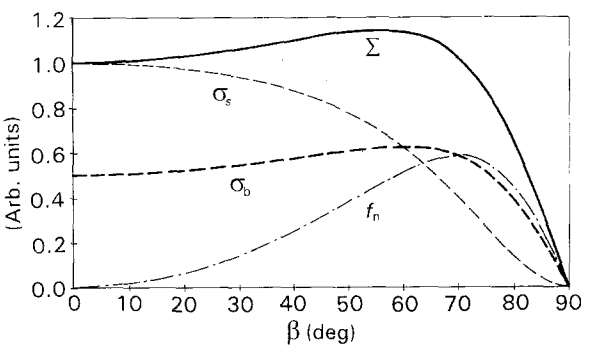

Figure 6 Surface stresses, sintering force and sintering stress versus dihedral angle.

force, Σ, might not coincide completely with S_{nn}. Further investigations on the kinetics of densification and creep are in progress [37] to evaluate the role of the gradients of stress-free chemical potentials on the mass-transport processes.

For the present, let us discuss some consequences of Equation 41.

If an external compressive force is applied to the sintering system, Equation 39 must be modified to take into account the work done by that force, i.e. $dW_{ext} = f_{ext}\, dL$. Thus the total true stress on the neck cross-section becomes

$$\Sigma = S_{nn} + \sigma_{ext} \tag{42}$$

where σ_{ext} is the (compressive) contribution of the external force. This result coincides with an assumption employed by other authors [13].

The magnitude of S_{nn}, as defined by the previous equations, can be modified by changing the state of strain in free surfaces and grain-boundary layers. This mechanism can be expected whenever a gaseous phase is adsorbed at the free surface of the particles and then it is weakly dissolved into the first nearest layers. Experimental evidence of this possibility has been obtained for the sintering of MgO in the presence of $H_2O(v)$ [38, 39] and of CaO in the presence of CO_2 [40]. In both cases it has been proved that the gaseous phase catalysed the sintering process. Furthermore, another experiment concerning the sintering of MgO in the presence of CO_2 [17] showed that such a gas is not an efficient catalyst for the densification. Further experimental studies proved [41] that the CO_2 in this last case is adsorbed at the surface but is not dissolved in the nearest layers of the bulk.

From these experiments it can be inferred that a gaseous phase, to be a catalyst for the sintering process of ceramic powders, must not only be chemically adsorbed at the surface but also be slightly dissolved into the nearest layers behind the free-surface.

The solubility of the gaseous species into the bulk changes the vacancy concentrations and therefore can influence the kinetic and the thermodynamic terms of the mass-transport phenomena.

The theory illustrated here predicts that to change the sintering potential S_{nn}, the gaseous phase should change the excess vacancy concentrations. In other words, if the gaseous phase dissolves into the bulk reaching thermodynamic equilibrium, its effect as a catalyst should be expected to reduce.

Fig. 7 [42] plots the amount of water that dissolves into an MgO layer against $1/T$, in the temperature range 580–1000 K. At temperatures higher than 823 K the equilibrium solubility is reached, while for lower temperature, the water vapour can dissolve only under non-equilibrium conditions. It is interesting to observe that water vapour, in the range of temperatures where its dissolution occurs in non-equilibrium conditions; has a true catalytic effect on the densification process (Fig. 8) [39], while the densification rate is not so greatly affected by the gaseous phase at higher temperatures.

This experiment, although significant, should not be taken as concluding proof for the theory because, as

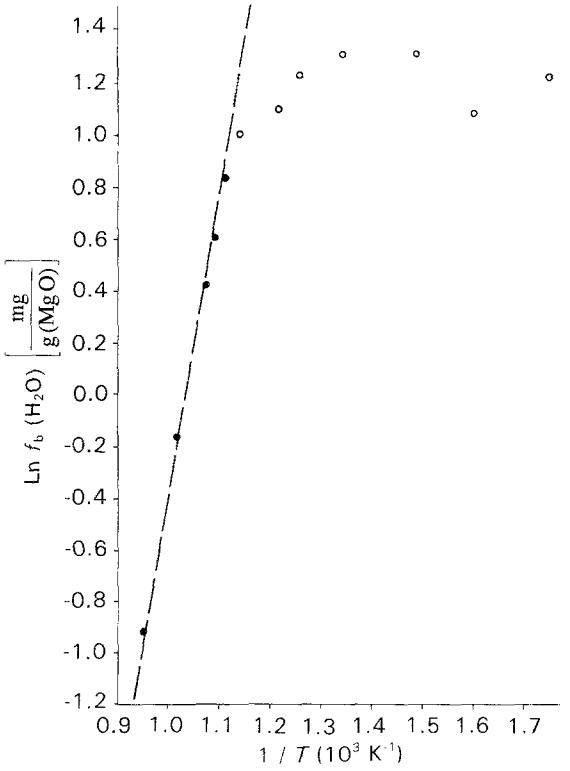

Figure 7 Water vapour dissolution into MgO versus $1/T$. (●) Equilibrium points ($T \geq 898$ K); (○) non-equilibrium points ($T \leq 898$ K).

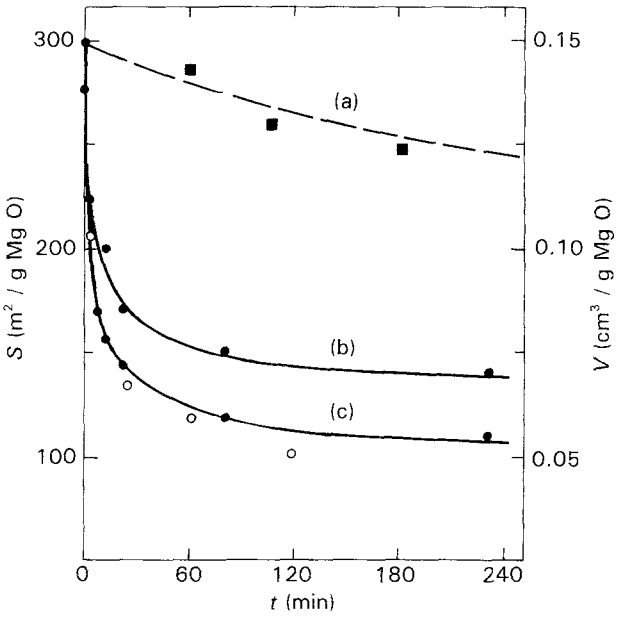

Figure 8 Evolution of nitrogen-accessible surface area (left scale) and pore volume (right scale) with time for sintering of MgO nanometric particles at $T = 823$ K, (a) in the absence of water vapour, (b, c) in the presence of water vapour.

the temperature becomes higher, the amount of dissolved water decreases. Nevertheless, the theory correctly predicts that the gaseous phase, to be a catalyst, must enter into the inner layers of the surface. In fact, if a gaseous phase is only adsorbed at the free surface, its effect would simply consist of reducing the surface tension, Γ_s, so that, according to the expression of S_{nn}

in Equation 40, the internal sintering stress would decrease.

Acknowledgements

The authors thank Professor A. W. Searcy for his valuable contributions in debating and improving the manuscript. This work has been supported by Centro Sviluppo Materiali, Rome, and, partially, by the Italian National Council of Researches under the Progetto Finalizzato Materiali Speciali per Tecnologie Avanzate.

Appendix 1. Displacement at the boundary of a spherical open membrane subjected to a given surfacial straining

With respect to a system of spherical coordinates, of which Θ represents the latitude, the surface strain in the case of meridian displacement, u_Θ, is given by

$$\varepsilon(\Theta) = (u_{\Theta,\Theta} + u_\Theta \operatorname{cotg}\Theta)/r_o \quad \text{(A1)}$$

In the present case, assuming $\varepsilon(\Theta)$ to be given by, say

$$\varepsilon(\Theta) = \varepsilon_o \cos\Theta \quad \text{(A2)}$$

Equation A1 is readily integrated to yield

$$u_\Theta = \varepsilon_o r_o/2 \sin\Theta + c_1/\sin\Theta \quad \text{(A3)}$$

Letting $c_1 = 0$ to avoid a singularity at $\Theta = \pi$, the displacement at the boundary (á circumference of radius a) ($\sin\Theta_o = a/r_o$, amounts to

$$\delta = \varepsilon_o a/2 \quad \text{(A4)}$$

Appendix 2. Elastic rigidity of a spherical open membrane loaded by unit meridian traction at a free boundary

The meridian displacement, $u_\Theta = d\phi/d\Theta$ must fulfil the differential equation [43]

$$\nabla^4\phi = 0 \quad \text{(A5)}$$

where Φ is a membrane function and the Laplace operator in spherical coordinates reads, in the case of meridian symmetry

$$\nabla^2 = (r_o^{-2}/\sin\Theta)d/d\Theta\,(\sin\Theta\, d/d\Theta) \quad \text{(A6)}$$

r_o being the radius of the sphere. The meridian membrane stress component is

$$\sigma_{\Theta\Theta} = 2G/r_o u_{\Theta,\Theta} + J/r_o(u_{\Theta,\Theta} + u_\Theta \operatorname{cotg}\Theta) \quad \text{(A7)}$$

G and J being the elasticities of the membrane, supposed to be elastically isotropic.

The solution of Equation A.5, after removal of singularities at $\Theta = \pi$, yields

$$u_\Theta = c_1 \operatorname{cotg}(\Theta/2) \quad \text{(A8)}$$

c_1 being an integration constant. Substituting in Equation A7 yields

$$\sigma_{\Theta\Theta} = G/r_o[c_1/\sin^2(\Theta/2)] + J(c^1/r_o) \quad \text{(A9)}$$

At the free boundary, $\Theta = \Theta_o$, $\sin\Theta_o = a/r_o \ll 1$, and $\sigma_{\Theta\Theta} = 1$; such conditions determine c_1

$$c_1 \approx a^2/4Gr_o \quad \text{(A10)}$$

Then, from Equation (A8), letting $\operatorname{cotg}(\Theta/2) \approx 2r_o/a$ for small a/r_o, we obtain

$$u_\Theta(\Theta_o) = \delta = a/2G \quad \text{(A11)}$$

from where the rigidity

$$k_1 = \delta^{-1} = 2G/a \quad \text{(A12)}$$

Appendix 3. Rigidity of a system of coupled membranes (refer to Figs 1 and 2b)

A radial unit traction at the neck cross-sectional ring produces a displacement which is a function of the rigidities of the two membranes and of the angles β_1, β_2. The unit traction has components in the two membranes, respectively

$$\sigma_1' = \sin\beta_2/\sin(\beta_1 + \beta_2) \quad \text{(A13a)}$$

$$\sigma_2' = \sin\beta_1/\sin(\beta_1/\beta_2) \quad \text{(A13b)}$$

The radial displacement at the neck can be calculated via the theorem virtual work, as

$$1\delta = \sigma_1'^2/k_1 + \sigma_2'^2/k_2 \quad \text{(A14)}$$

If $k_1 = k_2 = 2G_s/a$, Equation A14 yields the rigidity of the system

$$k_s = \delta^{-1} = \frac{2G_s}{a}\frac{\sin^2(\beta_1 + \beta_2)}{\sin^2\beta_1 + \sin^2\beta_2} \quad \text{(A15)}$$

Appendix 4. Rigidity of a circular plane membrane

A circular plane membrane of radius a, subjected to a unitary peripheral traction, undergoes a state of uniform strain

$$\varepsilon = u_{r,r} + u_r/r \approx 1/G_b \quad \text{(A16)}$$

where G_b is the elasticity of the membrane and u_r is the radial displacement. Integrating for the displacement and removing the singularity at $r = 0$, we obtain

$$u_r = r/2G_b \quad \text{(A17)}$$

from which the rigidity is

$$k_b = 2G_b/a \quad \text{(A18)}$$

References

1. A. G. EVANS, *J. Amer. Ceram. Soc.* **65** (1982) 497.
2. M. N. RAHAMAN, L. C. DE JONGHE and R. J. BROOK, *ibid.* **69** (1986) 53.
3. V. SERGO, Ceramica Acta. **2** (3) (1990) 37.
4. H. E. EXNER and P. BROSS, *Acta Metall.* **27** (1979) 1007.

5. *Idem*, in "Sintering and Catalysis", Vol. 10, edited by Kuczynski (Plenum Press, New York, 1975) p. 279
6. R. DEFAY and I. PRIGOGINE, "Surface tension and adsorption" (Longmans, London, 1966) p. 307 fll.
7. A. S. NOWICK and B. S. BERRY, "Anelastic relaxation in crystalline solids" (Academic Press, New York, 1972) p. 176 fll.
8. C. HERRING, in "The Physics of Powder Metallurgy", edited by W. E. Kingston (McGraw-Hill, Chicago, 1951) p. 165.
9. R. SHUTTLEWORTH, *Proc. Phys. Soc.* **63**, 5-A (1950) 444.
10. C. SOLLIARD and M. FLUELI, *Surface Sci.* **156** (1985) 487.
11. M. M. NICOLSON, *Proc. Roy. Soc. A* **228** (1955) 490.
12. P. VERGNON, M. ASTIER, D. BERUTO, G. BRULA and S. J. TEICHNER, *Rev. Int. Hautes Temp. Refract.* **9** (1972) 271.
13. L. C. DE JONGHE and M. N. RAHAMAN, *Acta Metall.* **36** (1988) 223.
14. R. M. CANNON and W. C. CARTER, *J. Amer. Ceram. Soc.* **72** (1989) 1550.
15. R. RAJ and R. K. BORDIA, *Acta Metall.* **32** (1984) 1003.
16. A.G. EVANS and C. H. HSUEH, *J. Am. Ceram. Soc.* **69** (1986) 444.
17. A. W. SEARCY, *J. Chem. Phys.* **81** (1984) 2489.
18. M. G. KIM, U. DAHMEN and A. W. SEARCY, *J. Amer. Ceram. Soc.* **70** (1987) 146.
19. A. E. GREEN, P. M. NAGHDI and W. L. WAINWRIGHT, *Arch. Rational Mech. Anal.* **20** (1965) 287.
20. E. and F. COSSERAT, "Théorie des corps déformables" (Dunod, Paris 1909) passim.
21. W. FLÜGGE, "Statik und Dynamik der Schalen" (Springer, Berlin, 1957) p. 10.
22. R. BALDACCI, "Scienza delle costruzioni II" (UTET, Torino, 1976) p. 113.
23. J. F. BELL, in "Handbuch der Physik", edited by D. Flügge, Vol. VIa/1, (Springer, Berlin, 1973).
24. J. J. GILMAN, *J. Appl. Phys.* **31** (1960) 2208.
25. L. LANDAU and E. LIFCHITZ, "Théorie de l'élasticité" (Mir, Moscow, 1967) p. 47.
26. F. F. LANGE and B. J. KELLETT, *J. Amer. Ceram. Soc.* **72** (1989) 725.
27. C. H. LUPIS, "Chemical Thermodynamics of Materials" (North Holland, Amsterdam, 1983) p. 367.
28. M. N. RAHAMAN and L. DE JONGHE, *J. Amer. Ceram. Soc.* **67** (1984) C-205.
29. M. CHU, L. C. DE JONGHE and M. N. RAHAMAN, *Acta Metall.* **37** (1989) 1415.
30. M. N. RAHAMAN and L. C. DE JONGHE, *J. Mater. Sci.* **22** (1987) 4326.
31. M. N. RAHAMAN, L. DE JONGHE and M. CHU, *J. Amer. Ceram. Soc.* **74** (1991) 514.
32. R. A. GREGG and F. N. RHINES, *Metall. Trans.* **4** (1973) 1365.
33. W. BEERE, *Acta Metall.* **23** (1975) 131.
34. *Idem, ibid.* **23** (1975) 139.
35. F. V. LENEL, in "IVth International Symposium on Science and Technology", Tokyo, Japan, November 1987.
36. F. F. LANGE, *J. Amer. Ceram. Soc.* **67** (1984) 83.
37. D. BERUTO, R. BOTTER and M. CAPURRO, unpublished (1992).
38. P. J. ANDERSON and P. L. MORGAN, *Trans. Farad. Soc.* **60** (1964) 930.
39. D. BERUTO, R. BOTTER and A. W. SEARCY, *J. Amer. Ceram. Soc.* **70** (1987) 155.
40. D. BERUTO, L. BARCO and A. W. SEARCY, *ibid.* **67** (1984) 512.
41. D. BERUTO, R. BOTTER and A. W. SEARCY, *J. Phys. Chem.* **91** (1987) 3578.
42. *Idem*, to be published in *J. Phys. Chem.* (1993).
43. A. E. H. LOVE, "A treatise on the mathematical theory of elasticity" (Cambridge University Press, Cambridge, 1983) p. 220 fll.

Received 27 April 1992
and accepted 24 February 1993